

Dalton Transactions

Accepted Manuscript



This is an *Accepted Manuscript*, which has been through the Royal Society of Chemistry peer review process and has been accepted for publication.

Accepted Manuscripts are published online shortly after acceptance, before technical editing, formatting and proof reading. Using this free service, authors can make their results available to the community, in citable form, before we publish the edited article. We will replace this *Accepted Manuscript* with the edited and formatted *Advance Article* as soon as it is available.

You can find more information about *Accepted Manuscripts* in the [Information for Authors](#).

Please note that technical editing may introduce minor changes to the text and/or graphics, which may alter content. The journal's standard [Terms & Conditions](#) and the [Ethical guidelines](#) still apply. In no event shall the Royal Society of Chemistry be held responsible for any errors or omissions in this *Accepted Manuscript* or any consequences arising from the use of any information it contains.



Journal Name

ARTICLE

Luminescence and energy transfers properties of novel $\text{Na}_{2.5}\text{Y}_{0.5}\text{Mg}_7(\text{PO}_4)_6: \text{R}$ ($\text{R}=\text{Eu}^{2+}$, Tb^{3+} and Mn^{2+}) phosphors

Received 00th January 20xx,
Accepted 00th January 20xx

DOI: 10.1039/x0xx00000x

www.rsc.org/

Yongyan Xu,^a Xueming Li,^{a,†} Wenlin Feng,^{b,c} Wulin Li,^d and Kai Zhang^e

A series of Eu^{2+} , Mn^{2+} and Tb^{3+} singly and co-doped $\text{Na}_{2.5}\text{Y}_{0.5}\text{Mg}_7(\text{PO}_4)_6$ phosphors have been prepared by solid-state reaction method. X-ray diffraction (XRD) patterns, scanning electron microscopy (SEM), transmission electron microscopy (TEM) and energy dispersive spectroscopy (EDS) have been used to characterise the crystal structure, morphology and composition of the as-prepared samples. The emission intensities of Mn^{2+} and Tb^{3+} are enhanced due to efficient energy transfer from Eu^{2+} to Mn^{2+} and Tb^{3+} in $\text{Na}_{2.5}\text{Y}_{0.5}\text{Mg}_7(\text{PO}_4)_6$. In addition, the energy transfer mechanisms between Mn^{2+} , Tb^{3+} and Eu^{2+} have been demonstrated. Similarly, white light emission in $\text{Na}_{2.5}\text{Y}_{0.5}\text{Mg}_7(\text{PO}_4)_6$ host can be realized by adjusting co-doped concentration of Eu^{2+} , Tb^{3+} and Mn^{2+} . The results indicate that the as-prepared phosphors have a great prospect as a phosphor-converted material for light-emitting diodes.

1. Introduction

White light-emitting diodes (WLEDs), a new generation lighting source, are considered as substitutes for traditional incandescent and fluorescent lamps because of their many advantages in high efficiency, energy saving, long operation time and environmental friendliness.^{1, 2} Nowadays, there are two general approaches to generate white light from LEDs.³ One approach is to mix emission light from several single-color LEDs, which can offer high luminous efficiency but requires complicated electronics resulting in limiting its general lighting applications.^{4, 5} The other approach is to combine a blue or near-ultraviolet (n-UV) LED chip with phosphors, known as phosphor-converted WLEDs (pc-WLEDs), which has aroused the researchers' enormous research interest attributing to the advantage of a compact package, a single power supply.^{6, 7} Currently, the most common method to obtain WLEDs is to combine a blue LED chip with $\text{Y}_3\text{Al}_5\text{O}_{12}:\text{Ce}^{3+}$ (YAG: Ce^{3+}) phosphors. However, this method suffers from the problems of low color rendering index and high correlated color temperature in lack of red composition, restricting their application.⁸ To overcome the

above disadvantages, a n-UV LED chip coated with tricolor (blue, green, red) phosphors is applied to preparing WLEDs. Unfortunately, the luminescence efficiency is low due to the reabsorption of emission colors among different phosphors.⁹ In addition, the device of WLEDs with multiple emitting components is very complicated and difficult to realize.¹⁰ To further improve the performance of WLEDs, many researches have carried out on single-phased white light-emitting phosphors, which is considered to be a promising method due to their merits of color stability and relatively simple fabrication process.¹¹⁻¹³

As we know, energy transfer between sensitizers and activators plays an important role in phosphors. Tb^{3+} and Mn^{2+} as activators are mainly used to provide green- and red-emitting light in fluorescent materials, nevertheless, their luminous efficiency is always lower upon n-UV excitation, since the absorption of Mn^{2+} and Tb^{3+} is spin- and parity-forbidden in n-UV region.¹⁴ Instead, Eu^{2+} ion, with strong capability to absorb n-UV light, can transfer its energy to activators in co-doped systems and then improve the luminous efficiency of activators.¹³⁻¹⁵ Phosphates as a matrix for fluorescent materials have attracted much attention in recent years, due to their outstanding low preparation temperature, thermal and chemical stability at high temperatures.¹⁶ Fallowite-like compounds form a small group of phosphates with chemical compositions approximating $\text{Na}_2\text{CaM}_7(\text{PO}_4)_6$ where M is alkali, alkaline earth, and rare earth.¹⁷ This structure contains a large variety of frameworks due to metal elements with various coordination polyhedra.¹⁸ In the point of view of fluorescent material design, fallowite-like compounds may offer more possibilities for the discovery of a new fluorescent material, benefiting from multiple substitution choices for foreign cations, such as rare earth ions, transition metal ions.

^a College of Chemistry and Chemical Engineering, Chongqing University, Chongqing, 400044, China

^b Department of Applied Physics, Chongqing University of Technology, Chongqing 400054, China

^c International Centre for Materials Physics, Chinese Academy of Sciences, Shenyang 110016, China

^d Chongqing Academy of Metrology and Quality Inspection, Chongqing 400020, China

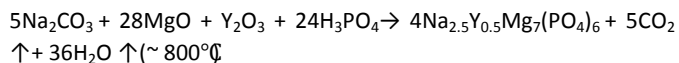
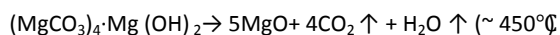
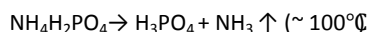
^e CET-College of Engineering and Technology, Southwest University, Chongqing 400716, China

† Corresponding author: lxm509cqu@163.com

However, as so far, few studies have reported luminescent properties of fillowite-like compounds. In 2010, a new phosphate, $\text{Na}_{2.5}\text{Y}_{0.5}\text{Mg}_7(\text{PO}_4)_6$ with fillowite-type was first synthesized via the flux method by Jerbi et al.¹⁸ However, there are still no information about its luminescent properties. Thus, in this paper, a series of novel $\text{Na}_{2.5}\text{Y}_{0.5}\text{Mg}_7(\text{PO}_4)_6$: R (R = Eu^{2+} , Tb^{3+} and Mn^{2+}) phosphors are synthesized via solid-state reaction method. Their luminescent properties and energy transfer mechanisms are also explored in detail.

2. Experimental

Powder samples were prepared by solid-state reaction method. The reagents were Na_2CO_3 [analytical reagent (A.R.), 99.9%], $\text{NH}_4\text{H}_2\text{PO}_4$ (A.R., 99.9%), $(\text{MgCO}_3)_4\cdot\text{Mg}(\text{OH})_2\cdot 5\text{H}_2\text{O}$ (A.R., 99.9%), Y_2O_3 (A.R., 99.9%), MnCO_3 (A.R., 99.9%), Tb_4O_7 (A.R., 99.99%), and Eu_2O_3 (A.R., 99.99%). Thermogravimetry and differential thermal analysis (TG-DTA) measurements were done prior to preparation of $\text{Na}_{2.5}\text{Y}_{0.5}\text{Mg}_7(\text{PO}_4)_6$ (abbreviated as NYMPO₄) compound under a nitrogen flow using a DTG-60H thermogravimetric analyzer at a heating rate of 10 °C/min. Fig. 1 shows the TG-DTA of NYMPO₄ compound. According to the TG curve, there are mainly four stages in the temperature monitoring range corresponding to the weight losses of the precursor via a four-step process. Considering the DTA curve, the four-step process can be depicted as follows:^{19,20}



According to the formula of NYMPO₄: $x\text{Eu}^{2+}$, $y\text{Mn}^{2+}$, $z\text{Tb}^{3+}$ (Eu^{2+} , Mn^{2+} and Tb^{3+} substitute for Na^+ , Mg^{2+} and Y^{3+} , respectively; $x=1-6$ mol%, $y=1-15$ mol% and $z=5-30$ mol%), stoichiometric amounts of reagents were mixed and ground sufficiently in an agate mortar. Then the mixtures were pre-fired at 450 °C for 3 h, 800 °C for 3 h in the air, and finally fired at 950 °C for 4 h in a N_2/H_2 (9:1) weak reducing atmosphere.

The crystal structures, morphology and composition of as-prepared samples were analyzed by using a X-ray diffractometer (XRD: XRD-6000), a field-emission scanning electron microscope (SEM: JSM-7800F) and a transmission electron microscope (TEM: JEM 2100). Diffuse reflectance spectra were carried on with a UV-Visible spectrophotometer (U-3010). Photoluminescence (excitation and emission) properties measurements were carried out on a Spectrofluorophotometer (RF-5301) with a 150 W xenon lamp as the excitation source at room temperature. The decay curves were determined on a Fluorescence Spectrometer (FLSP920). Photoluminescence quantum efficiency were measured directly by internal quantum efficiency measurement system (FLSP920).

3 Results and Discussion

3.1 Crystal structure, morphology and composition analysis

The morphology and composition of NYMPO₄ sample are presented by SEM and TEM images, as shown in Fig. 2. The SEM image shows that the sample presents a flake-like structure (Fig. 2 (a)), which is consistent with the TEM image (Fig. 2 (b)). Note that the HRTEM image exhibits the lattice fringes without clearly visible defects and dislocations, as shown in the inset of Fig. 2 (b), indicating that it is successful to prepared the crystals of NYMPO₄ host via solid-state reaction method, and it can be further proved with the XRD results. Fig. 2 (c) presents the EDS images of NYMPO₄ sample. The results show that the signals of Na, Y, Mg, P, and O are detected in NYMPO₄ sample. The bright spots of EDS mapping correspond to the presence of the elements Na, Y, Mg, P, and O, respectively, indicating that all elements are distributed uniformly throughout the whole area.

The XRD patterns of undoped NYMPO₄, NYMPO₄: 5% Eu^{2+} , NYMPO₄: 5% Tb^{3+} and NYMPO₄: 5% Mn^{2+} samples are shown in Fig. 3. Considering the structural details of NYMPO₄ have been reported by Jerbi et al., and not repeated in this paper.¹⁸ For NYMPO₄, the standard card is not available, hereby the undoped NYMPO₄ is used as the reference standard. It is clearly that the characteristic peaks are indexed to the pure phase of NYMPO₄, No other distinct impurities have been found, indicating that Eu^{2+} , Tb^{3+} , and Mn^{2+} ions are completely doped in NYMPO₄ host lattice without significant change in the crystal structure. On the basis of the comparison of the effective ionic radii of these cations with the given coordination number (Table 1), the Eu^{2+} , Mn^{2+} and Tb^{3+} ions are expected to occupy the Na^+ , Mg^{2+} and Y^{3+} ion sites in the NYMPO₄ host.²¹⁻²³

3.2 Photoluminescence properties

Fig. 4 shows the emission spectra of NYMPO₄: $x\text{Eu}^{2+}$ phosphors excited by 365 nm, as a function of Eu^{2+} concentration x ($x=0, 1\%, 2\%, 3\%, 4\%, 5\%$ and 6%). The emission spectra exhibit an asymmetric broad band in the 390- 550 nm range due to the $4f^65d^1 \rightarrow 4f^7$ transition of the Eu^{2+} ions. It is clearly that the emission intensity of Eu^{2+} varies as a function of Eu^{2+} concentration. The optimum Eu^{2+} concentration is 2 mol %, but somewhat higher values lead to concentration quenching attributed to the energy transfer among Eu^{2+} ions. Note that the emission peak of Eu^{2+} is red-shifted with increasing Eu^{2+} concentration. This is likely due to the crystal field strength increased with an increasing amount of Eu^{2+} since more Eu^{2+} ions replacing Na^+ site in NYMPO₄.²⁴

Fig. 5 (a) shows the diffuse reflectance spectra of NYMPO₄ host and NYMPO₄: Eu^{2+} phosphor, and the excitation and emission spectra of NYMPO₄: Eu^{2+} phosphor. The Stokes' shift of the Eu^{2+} emission is defined as the difference between the absorption energy of the

$4f^7[{}^8S_{7/2}] \rightarrow 4f^6[{}^7F_0]5d^1$ transition and the emission energy.²⁵ The Stokes' shift of NYMPO₄: Eu²⁺ is calculated to be 2076 cm⁻¹ by taking twice the energy difference between the zero phonon line energy and the energy of the emission peak.²⁶ It is clearly that the diffuse reflectance spectrum of NYMPO₄: Eu²⁺ phosphor presents a broad energy absorption band in the region of 300–420 nm, assigned to the $4f^7 \rightarrow 4f^65d^1$ transitions of Eu²⁺ ions, as compared with that of NYMPO₄ host. Monitored at 423 nm, the excitation spectrum of NYMPO₄: Eu²⁺ phosphor contains a broad band extending from 300 nm to 420 nm originating from $4f^7 \rightarrow 4f^65d^1$ transitions of Eu²⁺ ions, which matches well with its diffuse reflectance spectrum. This indicates that NYMPO₄: Eu²⁺ phosphor has a potential application in the field of n-UV LEDs, which is because its excitation band covers nearly the whole n-UV region.

The fluorescence decay curves of Eu²⁺ emission in the NYMPO₄: 5%Eu²⁺ phosphor under excitation at 365 nm and monitored at 423 nm are depicted in inset of Fig. 5 (a). The decay curves of Eu²⁺ ion are well fitted to a double exponential equation:

$$I(t) = A_1 \exp(-t/\tau_1) + A_2 \exp(-t/\tau_2) \quad (1)$$

where I is the luminescence intensity, A_1 and A_2 are constants, t is the time, τ_1 and τ_2 are lifetimes for exponential components. The average decay time (τ^*) can be determined by the following formula:²⁷

$$\langle \tau^* \rangle = (A_1 \tau_1^2 + A_2 \tau_2^2) / (A_1 \tau_1 + A_2 \tau_2) \quad (2)$$

Based on the Eq 2, the decay time of Eu²⁺ ion in NYMPO₄: 5%Eu²⁺ is determined to be ca. 3.55 μ s. There are three Na sites with different coordination numbers (CN = 6, 7 and 9) in NYMPO₄ host, the average bond length of Na (I)-O, Na (II)-O, Na (III)-O is 2.433 Å, 2.571 Å and 2.651 Å within polyhedral NaO6, NaO7 and NaO9, respectively.¹⁸ Theoretically, Eu²⁺ ion can randomly occupy Na⁺ sites and incorporated into the crystal structure of NYMPO₄ because the Eu²⁺ ionic radius ($r = 1.17$ Å for CN= 6, $r = 1.20$ Å for CN= 7, $r = 1.30$ Å for CN= 9) are similar to that of Na⁺ ($r = 1.02$ Å for CN= 6, $r = 1.12$ Å for CN= 7, $r = 1.24$ Å for CN= 9). The double exponential decay curve observed for Eu²⁺ indicates that Eu²⁺ is substituted at a minimum of two different coordinated sites, which is consistent with its structure.

In general, resonance type energy transfer mainly contains exchange interaction and electric multipolar interaction.²⁴ Exchange interaction usually works for a forbidden transition and the typical critical distance is about 5 Å, while electric multipolar interaction depends on the strength of the optical transitions and can occur for critical distance as large as 20 Å.^{28, 29} To further confirm the process of energy transfer between Eu²⁺ ions, here, the critical distance (R_c) is calculated based on the concentration quenching of Eu²⁺ ions. The value of R_c in NYMPO₄: Eu²⁺ phosphor can be estimated by using the following relation:³⁰

$$R_c \approx 2 \left(\frac{3V}{4\pi z x_c} \right)^{\frac{1}{3}} \quad (3)$$

where V is the volume of the unit cell, Z is the number of formula units per unit cell, x_c is the critical concentration. For NYMPO₄ host, $V = 8274.6 \text{ \AA}^3$, $Z = 18$ and $x_c = 2\%$. Based on Eq 3, R_c is estimated to be about 35 Å, with a value higher than 5 Å. Thus, energy transfer among Eu²⁺ ions in NYMPO₄: xEu²⁺ phosphors is attributed to electric multipolar interaction.

The emission and excitation spectra of NYMPO₄: Mn²⁺ phosphor are shown in Fig. 5 (c). Under 410 nm excitation, the emission spectrum of NYMPO₄: Mn²⁺ phosphor exhibits a weak broad band extending from 550 to 690 nm centered at 610 nm corresponding to the spin-forbidden ${}^4T_1 ({}^4G) \rightarrow {}^6A_1 ({}^6S)$ transition of Mn²⁺. Monitored by the emission at 610 nm, the excitation spectrum of NYMPO₄: Mn²⁺ phosphor contains three peaks located at 347, 364 and 410 nm, which correspond to the transitions from ${}^6A_1 ({}^6S)$ to ${}^4E ({}^4D)$, ${}^4T_2 ({}^4D)$ and [${}^4A_1 ({}^4G)$, ${}^4E ({}^4G)$] of Mn²⁺, respectively.³¹ Note that the excitation band at 410 nm overlaps with the emission band of Eu²⁺. Therefore, the resonant type energy transfer from Eu²⁺ to Mn²⁺ in NYMPO₄ host is expected, which will efficiently improve the luminous efficiency of Mn²⁺ through energy transfer.²⁸

Fig. 5 (d) shows the emission and excitation spectra of NYMPO₄: Tb³⁺ phosphor. It is clearly that the emission spectrum consists of several sharp peaks located at 488, 541, 585, and 621 nm, which is due to the ${}^5D_4 - {}^7F_{J=6, 5, 4, 3}$ transitions of Tb³⁺. In this case, the transitions of ${}^5D_3 - {}^7F_{6, 5, 4, 3}$ are not obvious due to weak intensity with respect to that of the ${}^5D_4 - {}^7F_{6, 5, 4, 3}$ and high Tb³⁺ concentration. Monitored at 541 nm, the excitation spectrum contains a band at 227 nm due to the spin-allowed transitions from the 4f⁸ ground state to the crystal-field-split components of the 4f⁷5d¹ configuration of Tb³⁺ ion, and several peaks in the 300–470 nm region, which correspond to the 4f-4f transition of Tb³⁺.³²

The emission and excitation spectra of NYMPO₄: 2%Eu²⁺, yMn²⁺ phosphors are exhibited in Fig. 6. Each emission spectrum consists of two broad bands located at 423 nm and at 610 nm, which have been corresponded to the emission band of Eu²⁺ ions and that of Mn²⁺ ions (Fig. 5). The emission intensity of Eu²⁺ decreases gradually as the Mn²⁺ concentration increases, whereas that of Mn²⁺ increases simultaneously; in this case, concentration quenching about Mn²⁺ is not observed. As shown in the inset of Fig. 6, it is also notable that the excitation spectrum of NYMPO₄: 2%Eu²⁺, 3%Mn²⁺ phosphor monitored with 610 nm (Mn²⁺ emission) is similar to that monitored with 423 nm (Eu²⁺ emission) except for luminous intensity. On the basis of above analysis, combining spectral overlapping between the excitation band of Mn²⁺ and the emission band of Eu²⁺ in NYMPO₄ host (Fig. 5), the existence of resonance type energy transfer from Eu²⁺ to Mn²⁺ in NYMPO₄ host is further confirmed.²⁹

According to Dexter's energy transfer formula of electric multipolar interaction and Reisfeld's approximation, the energy transfer

behavior from Eu^{2+} to Mn^{2+} ion can take place via exchange interaction and electric multipolar interaction.²⁵ The energy transfer mechanism of interaction between Eu^{2+} and Mn^{2+} can be obtained by the following equation:³³

$$I_0 / I \propto C^{\theta/3} \quad (4)$$

where C is the total doping concentration of the Eu^{2+} and Mn^{2+} ions; I_0 and I are the emission intensity of Eu^{2+} in the absence and presence of Mn^{2+} , respectively; θ ($=3, 6, 8$ and 10) corresponds to exchange interaction, dipole-dipole, dipole-quadrupole and quadrupole-quadrupole interaction, respectively. Fig. 7 shows the plots and linear fitting results of I_0/I versus $C^{\theta/3}$. This result reveals that exchange interaction is the best one among the fitting results, indicating that energy transfer from Eu^{2+} to Mn^{2+} ions in NYMPO_4 host is dominated by exchange interaction.

The energy transfer efficiency (η_T) can be calculated by the expression:³⁴ $\eta_T = 1 - I/I_0$ (where I_0 and I are consistent with above results, respectively.) Thus, the values of η_T are 16.5%, 33.4%, 40.3%, 47.5% and 53.6% for NYMPO_4 : 2% Eu^{2+} , $y\text{Mn}^{2+}$ phosphors as a function of Mn^{2+} concentration y ($y = 3\%, 6\%, 9\%, 12\%$ and 15%). It can be seen that the η_T increases gradually with the increase of Mn^{2+} concentration. Thus, energy transfer from Eu^{2+} to Mn^{2+} in NYMPO_4 host is efficient.

Fig. 8 (a) exhibits the excitation and emission spectra of NYMPO_4 : 2% Eu^{2+} , 20% Tb^{3+} phosphor. Monitored at 423 nm (Eu^{2+} emission), the excitation spectrum of NYMPO_4 : 2% Eu^{2+} , 20% Tb^{3+} shows a broad band extending from 300–420 nm which has been attributed to $4f^7 \rightarrow 4f^65d^1$ transition of Eu^{2+} , as shown in Fig. 5 (a). While monitored at 541 nm (Tb^{3+} emission), the excitation spectrum of NYMPO_4 : 2% Eu^{2+} , 20% Tb^{3+} phosphor contains an excitation band of Eu^{2+} and a characteristic excitation peak at 486 nm of Tb^{3+} , so which can be considered as one evidence for the occurrence of nonradiative energy transfer from Eu^{2+} to Tb^{3+} .²⁸ Excitation into Eu^{2+} band at 365 nm, the emission spectrum of NYMPO_4 : 2% Eu^{2+} , 20% Tb^{3+} phosphor contains both the emissions of Eu^{2+} and Tb^{3+} (${}^5\text{D}_{3,4} \rightarrow {}^7\text{F}_{6,5,4,3}$) where the ${}^5\text{D}_{3,4} \rightarrow {}^7\text{F}_{6,5,4,3}$ weak emission lines are overlapping with the broad Eu^{2+} emission band. With comparing excitation into Tb^{3+} band at 377 nm, the emission intensity of Tb^{3+} increases, whereas the emission intensity of Eu^{2+} decreases. The results further prove that Eu^{2+} as a sensitizer transfers its energy to Tb^{3+} in NYMPO_4 : Eu^{2+} , Tb^{3+} phosphors.²⁹ Fig. 8 (b) exhibits the variations of emission spectra of NYMPO_4 : 2% Eu^{2+} , $z\text{Tb}^{3+}$ ($z = 0, 5\%, 10\%, 15\%, 20\%, 25\%$ and 30%) phosphors excited at 365 nm, as a function of z . It is clearly that the emission intensity of Eu^{2+} and Tb^{3+} ions varies regularly with increasing Tb^{3+} concentration. Note that the color tone has gradually changed from blue to yellow-green with increasing Tb^{3+} concentration, as shown in the inset of Fig. 8 (b). In addition, the emission intensity of Tb^{3+} increases, while that of Eu^{2+} decreases gradually with increasing Tb^{3+} concentration (Fig. 8 (c)). In this case, there is no concentration quenching until the Tb^{3+} concentration reaches at 30%, at which the η_T is ca. 78%. Results indicate the existence of higher energy transfer efficiency in

NYMPO_4 : 2% Eu^{2+} , $z\text{Tb}^{3+}$ phosphors. Fig. 8 (d) presents the decay curves of Eu^{2+} ion in NYMPO_4 : 2% Eu^{2+} , $z\text{Tb}^{3+}$ ($z = 0, 5\%$, $\lambda_{\text{ex}} = 365$ nm, $\lambda_{\text{em}} = 423$ nm). Based on the Eq 2, the decay time of Eu^{2+} ion in NYMPO_4 : 2% Eu^{2+} and NYMPO_4 : 2% Eu^{2+} , 5% Tb^{3+} is determined to be ca. 3.72 μs and 3.67 μs , respectively. It can be seen that the decay time of Eu^{2+} decreases with the presence of Tb^{3+} , with 0.05 μs difference, indicating the existence of nonradiative energy transfer from Eu^{2+} to Tb^{3+} .

According to the above results, NYMPO_4 : 2% Eu^{2+} , 20% Tb^{3+} phosphor presents blue-white emission, which is close to the white light region. To obtain high quality white light, introduction of red-emitting component in NYMPO_4 : 2% Eu^{2+} , 20% Tb^{3+} phosphor is an efficient approach, which will enhance the colour saturation. In addition, Mn^{2+} as an activator is mainly used to provide red-emitting light in fluorescent materials.³⁵ Fig. 9 shows the emission spectra of NYMPO_4 : 2% Eu^{2+} , 20% Tb^{3+} , $y\text{Mn}^{2+}$ ($y = 1\sim 10\%$) under 365 nm excitation. The emission spectra consist of three major emission bands in the entire visible spectral region, which have been attributed to the contributions of Eu^{2+} , Tb^{3+} , and Mn^{2+} , as discussed above. The color tone of NYMPO_4 : 2% Eu^{2+} , 20% Tb^{3+} , $y\text{Mn}^{2+}$ can be tuned from yellow-green light to the white light with increasing of Mn^{2+} concentrations.

The probably energy transfer process between Eu^{2+} and Tb^{3+} is as follows: when the nonradiative relaxation of the excited state ($4f^65d^1$) of Eu^{2+} happens, energy maybe translate to low excited state of Tb^{3+} . The initial population firstly relaxes to the ${}^5\text{D}_3$ level and then to the ${}^5\text{D}_4$ level, or direct relaxes to the ${}^5\text{D}_4$ level, finally through radiative transition relaxes into the ground ${}^7\text{F}_j$ levels. Meanwhile, the energy transition is an irreversible process as the energy level of the lowest excited state of Eu^{2+} is higher than that of ${}^5\text{D}_4$ level of Tb^{3+} . If Tb^{3+} ion content is higher, the process is more frequent. Thus, the emission intensity of Tb^{3+} ion will increase with increasing its concentration, meanwhile that of Eu^{2+} ion decrease. Meanwhile, the $4f^65d^1$ excited state of Eu^{2+} is also close to the (${}^4\text{A}_1, {}^4\text{E}$ (${}^4\text{G}$)) level of Mn^{2+} ions. Therefore, it is highly possible that energy transfers from the excited state of Eu^{2+} to the (${}^4\text{A}_1, {}^4\text{E}$ (${}^4\text{G}$)) level of Mn^{2+} . Then, the excited electron relaxes to the ${}^4\text{T}_1$ (${}^4\text{G}$) level through ${}^4\text{T}_2$ (${}^4\text{G}$) intermediate energy level in a nonradiative process, followed by a radiative transition from the ${}^4\text{T}_1$ (${}^4\text{G}$) level to the ground state of ${}^6\text{A}_1$ (${}^6\text{S}$), with a typical red emission of Mn^{2+} . In this system, Tb^{3+} or Mn^{2+} doped phosphors show low luminescence efficiencies under n-UV excitation due to the $4f-4f$ weak absorption for Tb^{3+} and the forbidden ${}^4\text{T}_1 \rightarrow {}^6\text{A}_1$ transition for Mn^{2+} . Moreover, there is no obvious overlap between the main emission peaks of Tb^{3+} and the excitation band of Mn^{2+} . Therefore, the possibility of energy transfer from Tb^{3+} to Mn^{2+} is very small, and it can be ignored generally. The energy transfer process is schematically illustrated in Fig. 10.

3.3 Quantum efficiency and CIE coordinates

Quantum efficiency (QE) is an important technological parameter for phosphors in application. The internal QE of the NYMPO_4 :

2%Eu²⁺, NYMPO₄: 2%Eu²⁺, 10%Mn²⁺, NYMPO₄: 2%Eu²⁺, 20%Tb³⁺ and NYMPO₄: 2%Eu²⁺, 20%Tb³⁺, 10%Mn²⁺ phosphors were determined as 54%, 48%, 44% and 26% under 365 nm excitation. The internal QE of NYMPO₄: 2%Eu²⁺, 20%Tb³⁺, 10%Mn²⁺ is low by comparing with other tri-doped phosphors. However, the QE of the present phosphor can be further improved by controlling the particle size, size distribution, morphology and crystalline defects through optimization of the processing condition.

Fig. 11 summarize the International Commission on Illumination (CIE) chromaticity diagram of the NYMPO₄: 2%Eu²⁺, zTb³⁺, yMn²⁺ phosphors under 365 nm excitation. The corresponding CIE chromaticity coordinates (x, y) of NYMPO₄: 2%Eu²⁺, zTb³⁺, yMn²⁺ phosphors vary systematically from (0.18, 0.06) to (0.25, 0.12) with increasing Mn²⁺ concentration and from (0.16, 0.03) to (0.22, 0.36) with increasing Tb³⁺ concentration. Furthermore, from the introduction of Mn²⁺ in NYMPO₄: 2%Eu²⁺, 20%Tb³⁺ phosphor, the corresponding chromaticity coordinates (x, y) change from (0.25, 0.47) to (0.30, 0.33). As can be seen from the illustration in the insert of Fig. 11, the phosphor excited by 365 nm light exhibits white emitting-light, which indicates that this kind of novel phosphor can be used as a potential candidate for n-UV LEDs.

Conclusions

In summary, a series of Eu²⁺, Mn²⁺ and Tb³⁺ singly and co-doped NYMPO₄ phosphors have been synthesized by solid-state reaction. The optimal doping concentration of Eu²⁺ is x = 2%, R_c is estimated to be 35 Å. The emission intensities of Mn²⁺ and Tb³⁺ can be enhanced by co-doping of Eu²⁺ in NYMPO₄ host. The energy transfer processes between Eu²⁺ and Mn²⁺/Tb³⁺ have been investigated in detail. The energy transfer mechanism between Eu²⁺ and Mn²⁺ has been demonstrated to be the exchange interaction, and η_T is ca. 55% at y=15%. In NYMPO₄: Eu²⁺, Tb³⁺, the energy transfer between Eu²⁺ and Tb³⁺ mainly depends on nonradiative transition through the excited state of Eu²⁺ to the ⁵D_{3,4} level of Tb³⁺. Moreover, the color tone from blue to white light region can be obtained by adjusting the ratio of Eu²⁺, Tb³⁺ and Mn²⁺ concentration. The exploration about novel NYMPO₄: Eu²⁺, Tb³⁺, Mn²⁺ phosphors may provide a new option to design and fabricate n-UV LEDs.

Acknowledgements

This project is supported by the National Natural Science Foundation of China (No.61271059), the Natural Science Foundation Project of Chongqing (No. 2010BB4246), the Fundamental Research Funds for the Central Universities (No. CDJXS12220005) and the Sharing Fund of Chongqing University's Large-scale Equipment.

References

- 1 P. Waltreit, O. Brandt, A. Trampert, H. T. Grahn, J. Menniger, M. Ramsteiner, M. Reiche, & K. H. Ploog, *Nature*, 2000, 406, 865-868.
- 2 C. C. Lin, & R. S. Liu, *The Journal of Physical Chemistry Letters*, 2011, 2, 1268-1277.
- 3 K. N. Shinde, & S. J. Dhoble, *Critical Reviews in Solid State and Materials Sciences*, 2014, 39, 459-479.
- 4 M. M. Shang, G. G. Li, D. L. Geng, D. M. Yang, X. J. Kang, Y. Zhang, H. Z. Lian, & J. Lin, *The Journal of Physical Chemistry C*, 2012, 116, 10222-10231.
- 5 M. M. Shang, G. G. Li, X. J. Kang, D. M. Yang, D. L. Geng, & J. Lin, *ACS Applied Materials & Interfaces*, 2011, 3, 2738-2746.
- 6 D. P. Dutta, & A. K. Tyagi, *Solid State Phenomena*, 2009, 155, 113-143.
- 7 H. Jing, C. F. Guo, G. G. Zhang, X. Y. Su, Z. Yang, & J. H. Jeong, *Journal of Materials Chemistry*, 2012, 22, 13612-13618.
- 8 M. M. Jiao, Y. C. Jia, W. Lü, W. Z. Lv, Q. Zhao, B. Q. Shao, & H. P. You, *Journal of Materials Chemistry C*, 2014, 2, 4304-4311.
- 9 W. Lü, N. Guo, Y. C. Jia, Q. Zhao, W. Z. Lv, M. M. Jiao, B. Q. Shao, & H. P. You, *Inorganic chemistry*, 2013, 52, 3007-3012.
- 10 J. S. Hou, W. Z. Jiang, Y. Z. Fang, & F. Q. Huang, *Journal of Materials Chemistry C*, 2013, 1, 5892-5898.
- 11 C. H. Huang, T. M. Chen, W. R. Liu, Y. C. Chiu, Y. T. Yeh, & S. M. Jang, *ACS Applied Materials & Interfaces*, 2010, 2, 259-264.
- 12 X. Chen, P. P. Dai, X. T. Zhang, C. Li, S. Lu, X. L. Wang, Y. Jia, & Y. C. Liu, *Inorganic chemistry*, 2014, 53, 3441-3448.
- 13 M. M. Shang, C. X. Li, & J. Lin, *Chemical Society Reviews*, 2014, 43, 1372-1386.
- 14 J. McKittrick, M. E. Hannah, A. Piquette, J. K. Han, J. I. Chol, M. Anc, M. Galvez, H. Lugauer, J. B. Talbot, & K. C. Mishra, *ECS Journal of Solid State Science and Technology*, 2013, 2, 3119-3131.
- 15 C. F. Guo, X. Ding, L. Luan, & Y. Xu, *Sensors and Actuators B* 2010, 143, 712-715.
- 16 X. G. Zhang, J. L. Zhang, & M. L. Gong, *Optical Materials*, 2014, 36, 850-853.
- 17 S. S. Hu & W. J. Tang, *Journal of Materials Science*, 2013, 48, 5840-5845.
- 18 H. Jerbi, M. Hidouri, & M. B. Amara, *Journal of Rare Earths*, 2010, 28, 481-487.
- 19 Y. C. Wang, Z. M. Du, X. M. Cong, & X. L. Tian, *Applied Chemical Industry*, 2008, 37, 657-660.
- 20 J. H. Jeong, M. Jayasimhadri, H. S. Lee, K. W. Jang, S. S. Yi, J. H. Jeong, & C. D. Kim, *Physica B*, 2009, 404, 2016-2019.
- 21 Z. G. Xia, Y. Y. Zhang, M. S. Molokeev, & V. V. Atuchin, *The Journal of Physical Chemistry C*, 2013, 117, 20847-20854.
- 22 L. Wu, B. Wang, Y. Zhang, L. Li, H. R. Wang, H. Yi, Y. F. Kong, & J. J. Xu, *Dalton Transactions*, 2014, 43, 13845-13851.
- 23 F. Zhang, Y. H. Wang, J. Zhang, B. T. Liu, Y. Wen, & Y. Tao, *Electrochemical and Solid-State Letters*, 2011, 14, J16-J18.
- 24 K. Li, J. Fan, X. Y. Mi, Y. Zhang, H. Z. Lian, M. M. Shang, & J. Lin, *Inorganic chemistry*, 2014, 53, 12141-12150.
- 25 S. Y. Zhang, Y. L. Huang, L. Shi, & H. J. Seo, *J. Phys.: Condens. Matter*, 2010, 22, 235402.
- 26 D. L. Wei, Y. L. Huang, & H. L. Seo, *Materials Research Bulletin*, 2013, 48, 3614-3619.
- 27 H. Yu, D. G. Deng, D. T. Zhou, W. Yuan, Q. E. Zhao, Y. J. Hua, S. L. Zhao, L. H. Huang, & S. Q. Xu, *Journal of Materials Chemistry C*, 2013, 1, 5577-5582.
- 28 X. Y. Huang, S. Y. Han, W. Huang, & X. G. Liu, *Chemical Society Reviews*, 2013, 42, 173-201.
- 29 D. G. Deng, H. Yu, Y. Q. Li, Y. J. Hua, G. H. Jia, S. L. Zhao, H. P. Wang, L. H. Huang, Y. Y. Li, C. X. Li, & S. Q. Xu, *Journal of Materials Chemistry C*, 2013, 1, 3194-3199.
- 30 G. Blasse, *Philips Res. Rep.* 1969, 24, 131-144.

ARTICLE

Journal Name

- 31 H. Yu, D. G. Deng, D. T. Zhou, W. Yuan, Q. E. Zhao, Y. J. Hua, S. L. Zhao, L. H. Huang, & S. Q. Xu, *Journal of Materials Chemistry C*, 2013, 1, 5577-5582.
- 32 K. Li, D. L. Geng, M. M. Shang, Y. Zhang, H. Z. Lian, & J. Lin, *Journal Physical Chemistry C*, 2014, 118, 11026-11034.
- 33 Y. H. Wang, M. G. Brik, P. Dorenbos, Y. Huang, Y. Tao, & H. B. Liang, *The Journal of Physical Chemistry C*, 2014, 118, 7002-7009.
- 34 D. L. Dexter & James H. Schulman, *The Journal of Chemistry Physical*, 1954, 22, 1063-1070 .
- 35 Y. Chen, Y. Li, J. Wang, M. M. Wu, & C. X. Wang, *Journal Physical Chemistry C* 2014, 118, 12494-12499.
- 36 N. Guo, Y. J. Huang, M. Yang, Y. H. Song, Y. H. Zheng, & H. P. You, *Physical Chemistry Chemical Physics*, 2011, 13, 15077-15082.
-

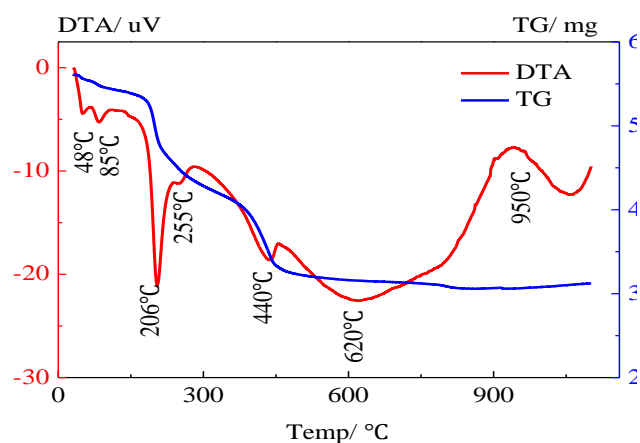
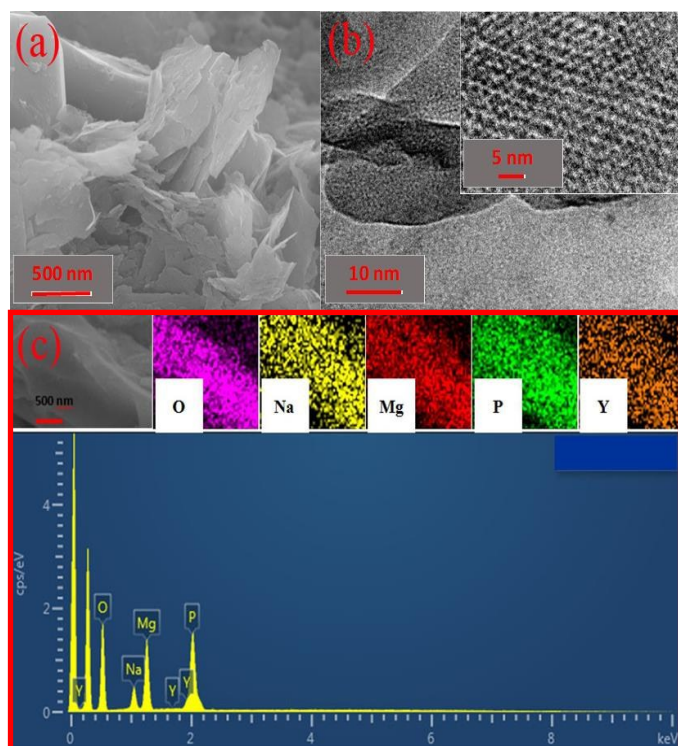
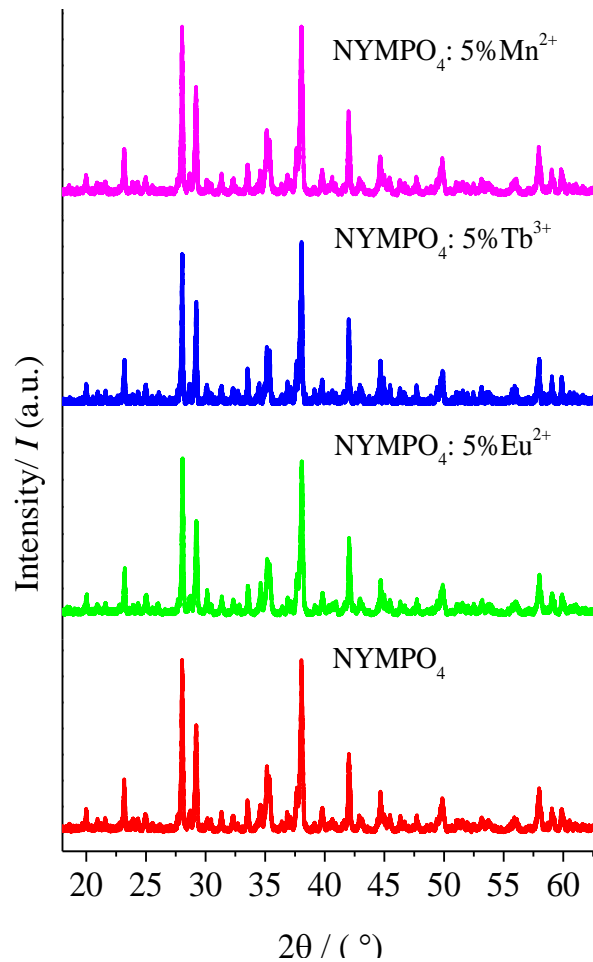
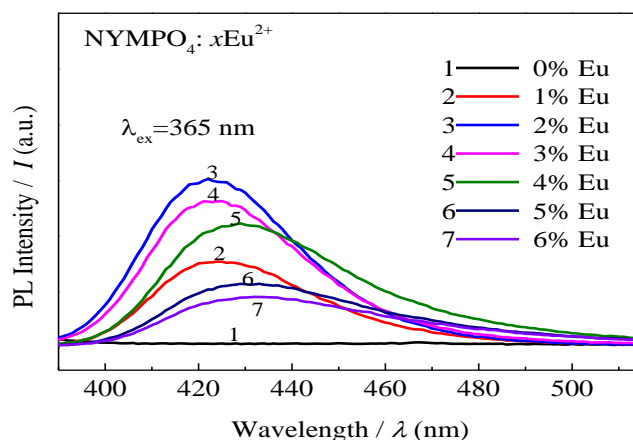
Fig. 1 Thermalanalysis of NYMPO₄.Fig. 2 (a) SEM image, (b) TEM/ HRTEM images and (c) EDS images of NYMPO₄ host.Fig. 3 XRD pattern of undoped NYMPO₄ host, NYMPO₄: 5%Eu²⁺, NYMPO₄: 5%Tb³⁺ and NYMPO₄: 5%Mn²⁺.

Fig. 4 The emission spectra ($\lambda_{\text{ex}}=365$ nm) of $\text{NYMPO}_4: x\text{Eu}^{2+}$ with varying Eu^{2+} concentration.

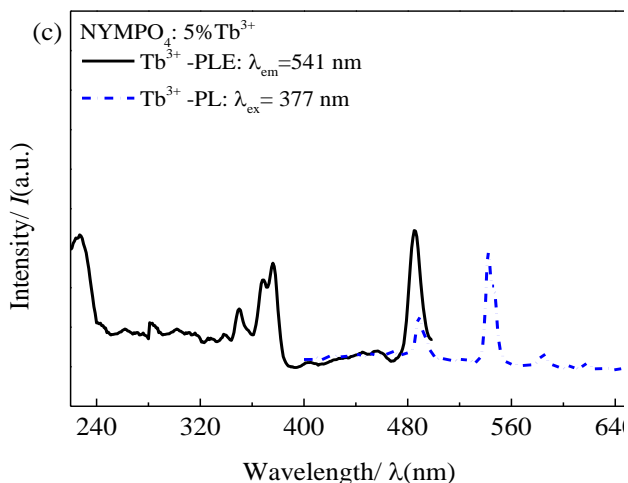
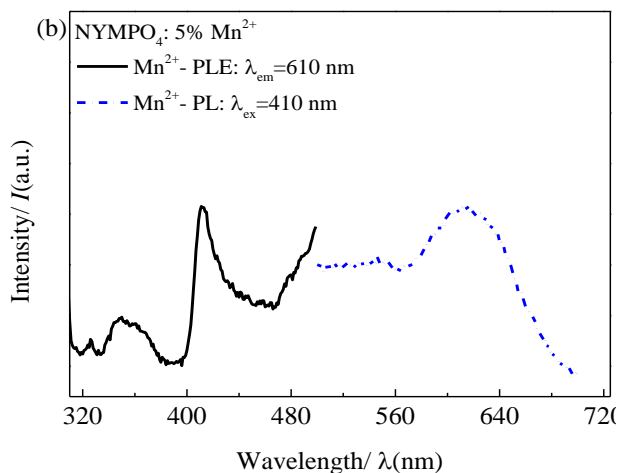
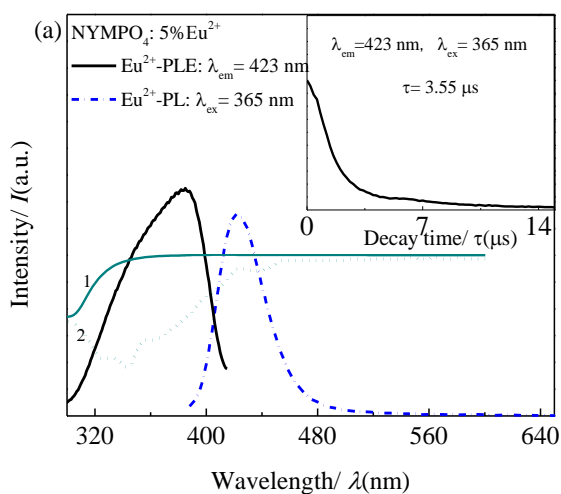


Fig. 5. (a) The diffuse reflectance spectra of NYMPO_4 (1- solid line) and $\text{NYMPO}_4: 5\%\text{Eu}^{2+}$ (2- dotted line), the PL/PLE spectra of $\text{NYMPO}_4: 5\%\text{Eu}^{2+}$. The inset shows the decay curve of $\text{NYMPO}_4: 5\%\text{Eu}^{2+}$ phosphor. The PL/PLE spectra of (b) $\text{NYMPO}_4: 5\%\text{Mn}^{2+}$ and (c) $\text{NYMPO}_4: 5\%\text{Tb}^{3+}$ phosphor.

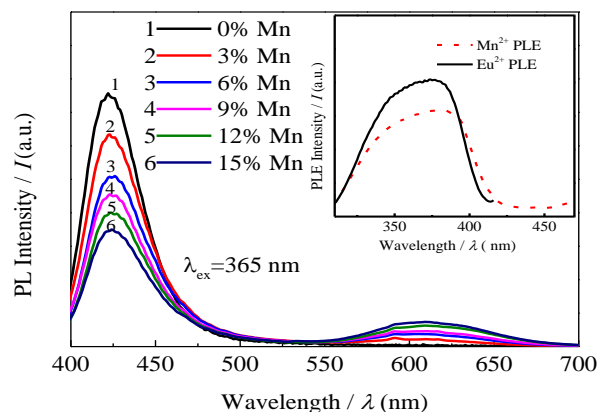


Fig. 6. The emission spectra of $\text{NYMPO}_4: 2\%\text{Eu}^{2+}, y\text{Mn}^{2+}$ phosphors with varying Mn^{2+} concentration. The inset shows the excitation spectra of $\text{NYMPO}_4: 2\%\text{Eu}^{2+}, 3\%\text{Mn}^{2+}$ phosphor.

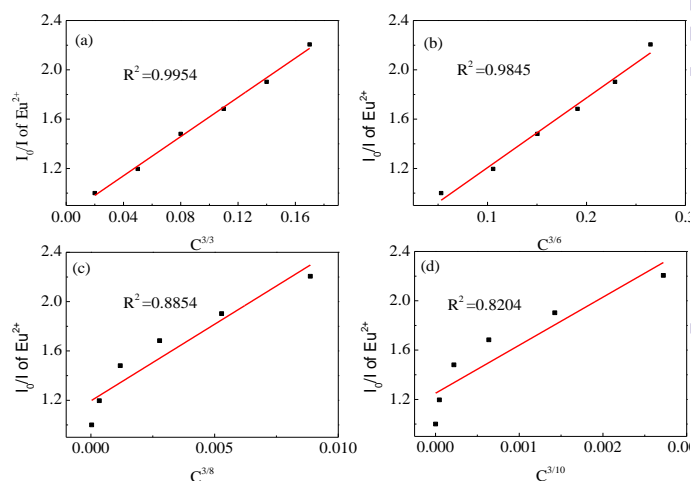
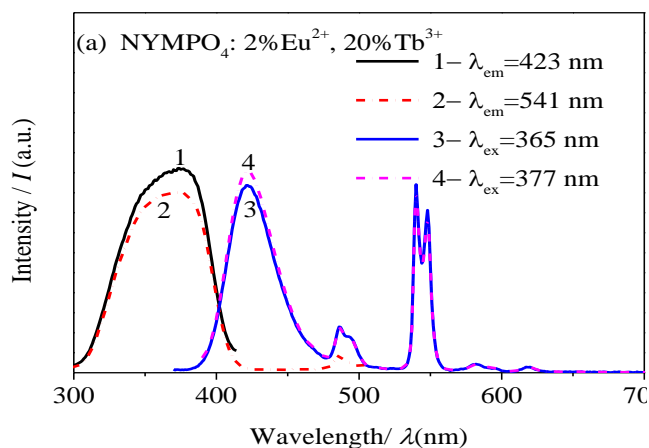


Fig. 7. Dependence of I_0/I on $C^{\theta/3}$ on the exponent (a) $\theta=3$, (b) $\theta=6$, (c) $\theta=8$ and (d) $\theta=10$.



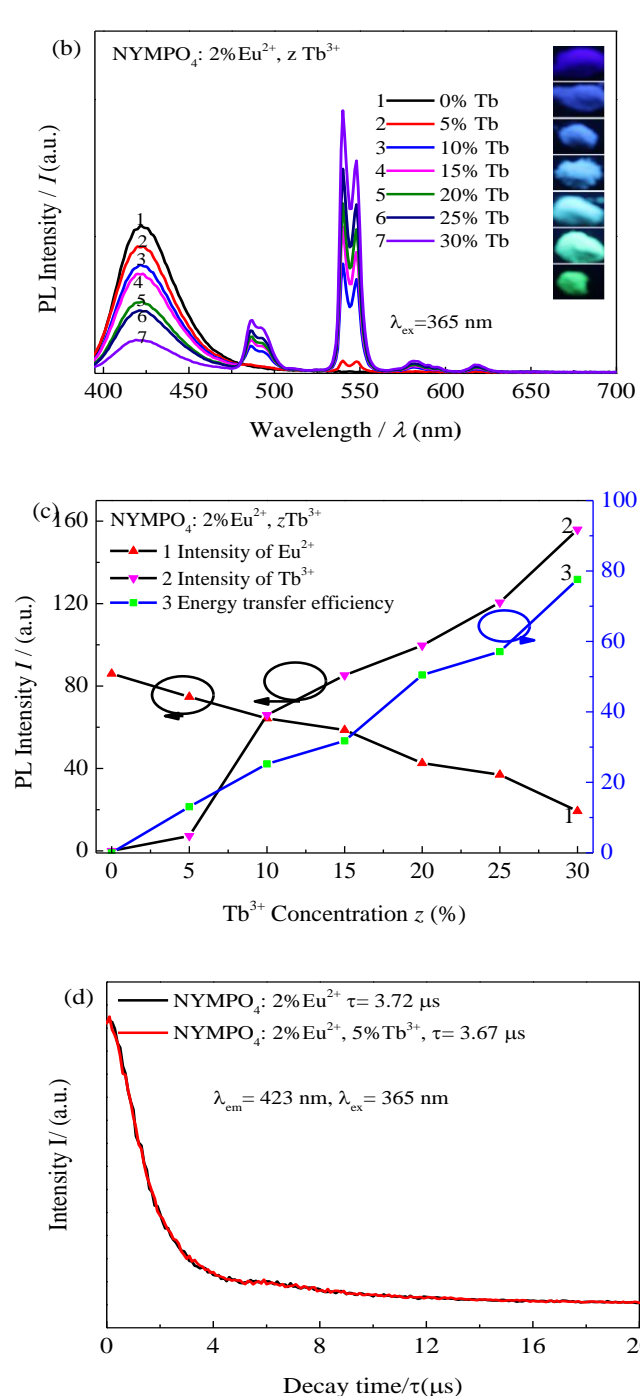


Fig. 8. (a) The excitation and emission spectra of NYMPO₄: 2%Eu²⁺, 20%Tb³⁺ phosphor. (b) The emission spectra (λ_{ex} = 365 nm) of NYMPO₄: 2%Eu²⁺, zTb³⁺ (z = 0, 5, 10, 15, 20, 25 and 30%) as a function of Tb³⁺ concentration z. (c) The dependence of emission intensity of Eu²⁺ and Tb³⁺, and energy transfer efficiency between Eu²⁺ and Tb³⁺ on Tb³⁺ concentration. (d) The decay curves of NYMPO₄: 2%Eu²⁺, zTb³⁺ (z = 0 and 5%) phosphor.

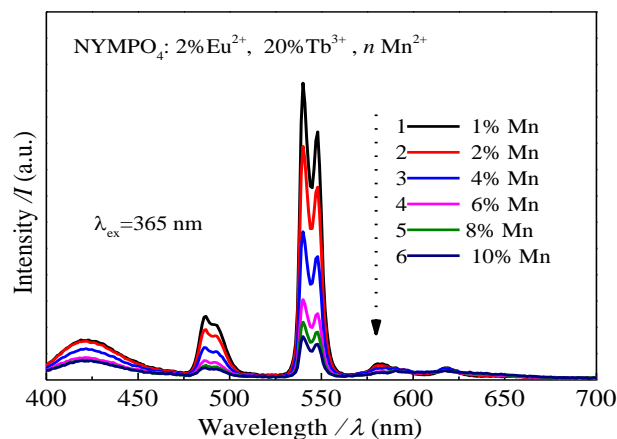


Fig. 9. The emission spectra of NYMPO₄: 2%Eu²⁺, 20%Tb³⁺, yMn²⁺ (y = 1~10%) phosphors under 365 nm excitation.

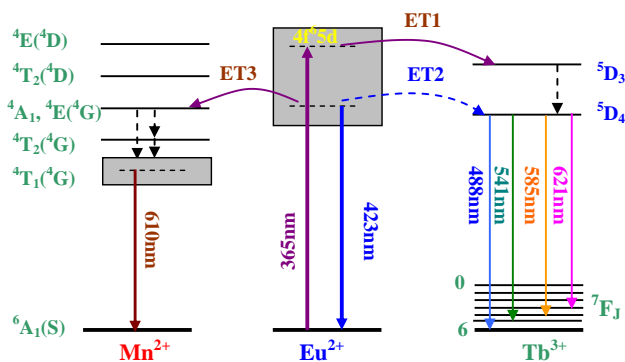


Fig. 10. Simple energy level scheme for energy transfer process in NYMPO₄ host.

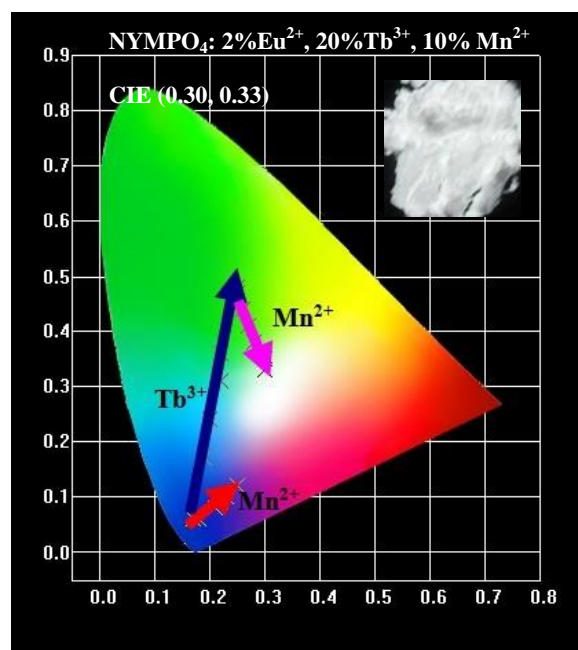


Fig. 11. CIE chromatic coordinates of NYMPO₄: 2%Eu²⁺, zTb³⁺, yMn²⁺ phosphors.

Table. 1 Ionic radii(Å) for given coordination number (CN) of Na⁺, Mg²⁺, Y³⁺, Eu²⁺, Mn²⁺ and Tb³⁺ ions.

Ions	Ionic radii (Å)				
	CN=5	CN=6	CN=7	CN=8	CN=9
Na ⁺		1.02	1.12		1.24
Mg ²⁺	0.66	0.72			
Y ³⁺		0.90		1.02	
Eu ²⁺		1.17	1.20		1.30
Mn ²⁺	0.75	0.83			
Tb ³⁺		0.92		1.04	

Graphical abstract

A color-tunable emission in $\text{Na}_{2.5}\text{Y}_{0.5}\text{Mg}_7(\text{PO}_4)_6$ phosphors can be realized by adjusting the ratio of Eu^{2+} , Tb^{3+} and Mn^{2+} concentration.

